Turkish Journal of Earth Sciences (Turkish J. Earth Sci.), **Vol. 16**, 2007, pp. 523–539. *Copyright ©TÜBİTAK*

Jurassic Volcanism in the Eastern Pontides: Is it Rift Related or Subduction Related?

CÜNEYT ŞEN
Department of Geological Engineering, Karadeniz Technical University, TR–61080 Trabzon, Turkey
(E-mail: csen@ktu.edu.tr)

Abstract: The Jurassic volcanic rocks in the centre of the northern zone (south of Trabzon City) provide important constraints on the evolution of Pontides. The investigated volcanic rocks form a transitional series between tholeiitic and calc-alkaline, and is dominated by basalt, basaltic andesite and andesite. Geochemically, they are enriched in LILE and LREE contents and depleted in HFSE [$(La/Yb)_N$= 2.2 – 8.5; $(Nb/La)_N$= 0.1 – 0.77)] compared to mid-ocean ridge basalts and have radiogenic Nd isotope ratios of εNd(*210 Ma*)= -0.72 to 3.24. These trace element and isotope data suggest that these rocks were derived from low degrees of partial melting of spinel lherzolite that was metasomatized by subduction-related fluids and further underwent a degree of fractional crystallization in magma chambers before being extruded at the surface.

Key Words: Eastern Pontides, geochemistry, Sr-Nd isotopes, Jurassic, basalt, Turkey

Doğu Pontid'lerde Jura Volkanizması: Rift mi yoksa Yitim ilişkili mi?

Özet: Pontidlerin kuzey zonunun orta kısmında (Trabzon'un hemen güneyinde) yüzeylenen Jura volkanitleri, Pontidlerin evrimine ilişkin önemli veriler sunar. Bu volkanik kayaçlar toleyitlerle kalk-alkalen kayaçlar arasında geçiş sunar ve çoğunlukla bazalt, bazaltik-andezit ve andezit bileşimindedir. Jeokimyasal özellikleri bakımından, okyanus ortası sırtı bazaltlarına göre büyük iyon çaplı ve hafif nadir toprak elelmentlerce zenginleşmişler ve yüksek alan enerjili elementlerce fakirleşmişlerdir [(La/Yb)cn= 2.2 – 8.5; (Nb/La)n= 0.1 – 0.77)] ve radyojenik Nd izotop oranları εNd(210 *Ma*)= -0.72 to 3.24'dür. İz element ve izotop verileri bu kayaçların, yitim ilişkili sıvılarca metasomatizmaya uğratılmış spinel lerzolitin düşük dereceli bölümsel ergimesi sonucu oluştuğunu ve yüzeye akmadan önce bir magma odasında fraksiyonel kristallenmeye uğradığını önermektedir.

Anahtar Sözcükler: Doğu Pontidler, jeokimya, Sr-Nd izotopları, Jura, basalt, Türkiye

Introduction

The study area is in the centre of the northern zone (Akın 1978; Gedikoğlu *et al.* 1978; Özsayar *et al.* 1981; Bektaş *et al.* 1999) of the Eastern Pontides (Ketin 1966; Yılmaz *et al.* 1997). The Pontides tectonic belt of northern Turkey tectonically combines three different sectors: the western Pontides, the central Pontides and the Eastern Pontides (Yılmaz *et al.* 1997). Although their general evolution seems similar, all three sectors have their own distinct evolution stories.

The orogenic belt of the Eastern Pontides is subdivided into two E–W-trending tectonostratigraphic zones: the northern and southern zones. The northern zone of the Eastern Pontides is dominated by Senonian and Middle Eocene volcanic and volcaniclastic rocks. In contrast, pre-Senonian rocks are widely exposed in the southern zone of the Eastern Pontides, which occupied a fore-arc position during the Senonian and underwent much more intensive deformation than the northern zone during the Early Tertiary continental collision (Okay & Şahintürk 1997). The boundary between these zones approximately follows the Niksar-Torul-İspir line (Okay & Şahintürk 1997; Bektaş *et al.* 1999).

It is now agreed that the tectonic evolution of Eastern Pontides between the Late Palaeozoic and mid-Jurassic was very similar to that of other sectors of the Pontides (Yılmaz *et al.* 1997). But the location of the Palaeotethyan suture and its subduction polarity is still disputed (Ustaömer & Robertson 1997). In the light of recent studies, Ustaömer & Robertson (1997) reviewed two fundamentally different views. (i) One school considered that the north Tethyan margin was passive until the Late Jurassic, and hence the Palaeotethys Ocean was subducted southward under the active margin of

Gondwana during the Palaeozoic (Dewey *et al.* 1973; Şengör *et al.* 1984; Şengör 1987). During the subduction, a continental sliver rifted off as a result of back-arc extension, opening a new ocean (Neotethys) to the south. This continental sliver was accreted to Laurasia by the Late Jurassic. (ii) The second school regarded the southern margin of Eurasia as an active continental margin associated with terrane displacement, marginal basin formation, and arc genesis (Adamia *et al.* 1977; Robertson & Dixon 1984; Dercourt *et al.* 1993). In this model, only one progressively evolving Tethys Ocean existed. Continental slivers rifted off Gondwana, drifted northwest, and were later accreted to the southern margin of Eurasia. In the same study, Ustaömer & Robertson (1997) proposed a scenario in which 'north-facing half-grabens' formed in the north and were filled by turbiditic sediments, debris flows and limestone blocks derived from the carbonate platform in the Central Pontides. Early Cretaceous extension developed above a northward-dipping subduction zone and was a precursor to opening of the Black Sea as a back-arc basin in the Late Mesozoic–Early Tertiary'.

Yılmaz *et al.* (1997) suggested that the Karakaya marginal basin was generated behind the volcanic arc during southward subduction in the Triassic. After closure of the Karakaya Basin by continuing subduction in the latest Triassic, the Neotethys (the İzmir–Ankara–Erzincan Ocean) opened up as a new basin during the Liassic. On the other hand, Okay (2000) and Okay *et al.* (2002) thought that an Early–Middle Triassic oceanic plateau (Nilüfer unit) collided with and accreted to the southern continental margin of Laurasia. They concluded that this caused a short-lived orogeny which was completed by the Early Jurassic. However, Golonka (2004) stated that during Late Triassic–Early Jurassic time, several microplates were sutured to the Eurasian margin, closing the Palaeotethys Ocean. He stated that 'a Jurassic–Cretaceous north-dipping subduction boundary was developed along this new continental margin south of the Pontides'. Kazmin *et al.* (1986) also argued that Early Jurassic volcanism (even though it was not so widespread) was related to subduction of the Mesozoic Tethys oceanic crust, whereas Şengör & Yılmaz (1981) believed that most Lower Jurassic volcanic rocks in the Eastern Pontides are of oceanic tholeiite rather than island arc type and are related to Liassic rifting.

The Liassic rift is described by many researchers (Şengör & Yılmaz 1981; Görür *et al.* 1983; Bergougnan 1987; Yılmaz *et al.* 1996; Koçyiğit & Altıner 2002). Şengör & Yılmaz (1981) stated that the rift was filled by thick coarse clastic rocks, together with alkaline and tholeiitic lavas. It is also described as the North Anatolian Palaeorift (NAPR) by Koçyiğit & Altıner (2002) in northern Turkey and is interpreted as the south-facing passive continental margin of the northern Neotethys; it developed during the Hettangian. In this basin, the Liassic is characterized by rift-related sediments (Şengör & Yılmaz 1981; Görür *et al.* 1983; Bergougnan 1987; Yılmaz *et al.* 1996; Koçyiğit & Altıner 2002) and overlain by typical shelf carbonates. Readers are refereed to the most recent literature for information about the geology of Eastern Pontides (Okay & Şahintürk 1997; Ustaömer & Robertson 1997; Yılmaz *et al.* 1997; Arslan 2005, 2006; Dokuz & Tanyolu 2006; Topuz & Okay 2006; Topuz 2006 and references therein).

Early to Middle Jurassic time is represented by thick coarse clastic rocks, comprising volcanic rocks (tuff, pyroclastic rocks, lava), and interbedded clastic sedimentary rocks that make up a 2000-m-thick sequence on the Hercynian basement in the southern zone of Eastern Pontides. By contrast, in the northern zone the Jurassic is represented by lava flows and pyroclastic rocks. As seen from this summary, there is no agreement among the researchers about the tectonic setting of the Jurassic rocks. The present paper therefore presents the results of a detailed field, petrologic and geochemical study of the volcanic rocks and discusses their origin and tectonic significance in order to shed light on the tectonomagmatic evolution of the Eastern Pontides, and resolve the existing controversies.

Lithostratigraphy of Studied Locations

Field relationships were studied at the centre of the northern part of the Eastern Pontides, in an area south of Trabzon (Figure 1). The stratigraphic succession in the study area ranges from Jurassic to Quaternary (Yılmaz *et al.* 2005). Jurassic exposures are either bounded by NE–SW-trending transtensional faults (Figure 1) or are intruded by Cretaceous granitoids: the NE–SW-trending faults might have facilitated the emplacement of granitic intrusions.

A thick pillow lava sequence represents the basement in the İkisu Valley (Figure 2). Massive basaltic lava flows, intercalated with tuff horizons, cover the pillow lavas,

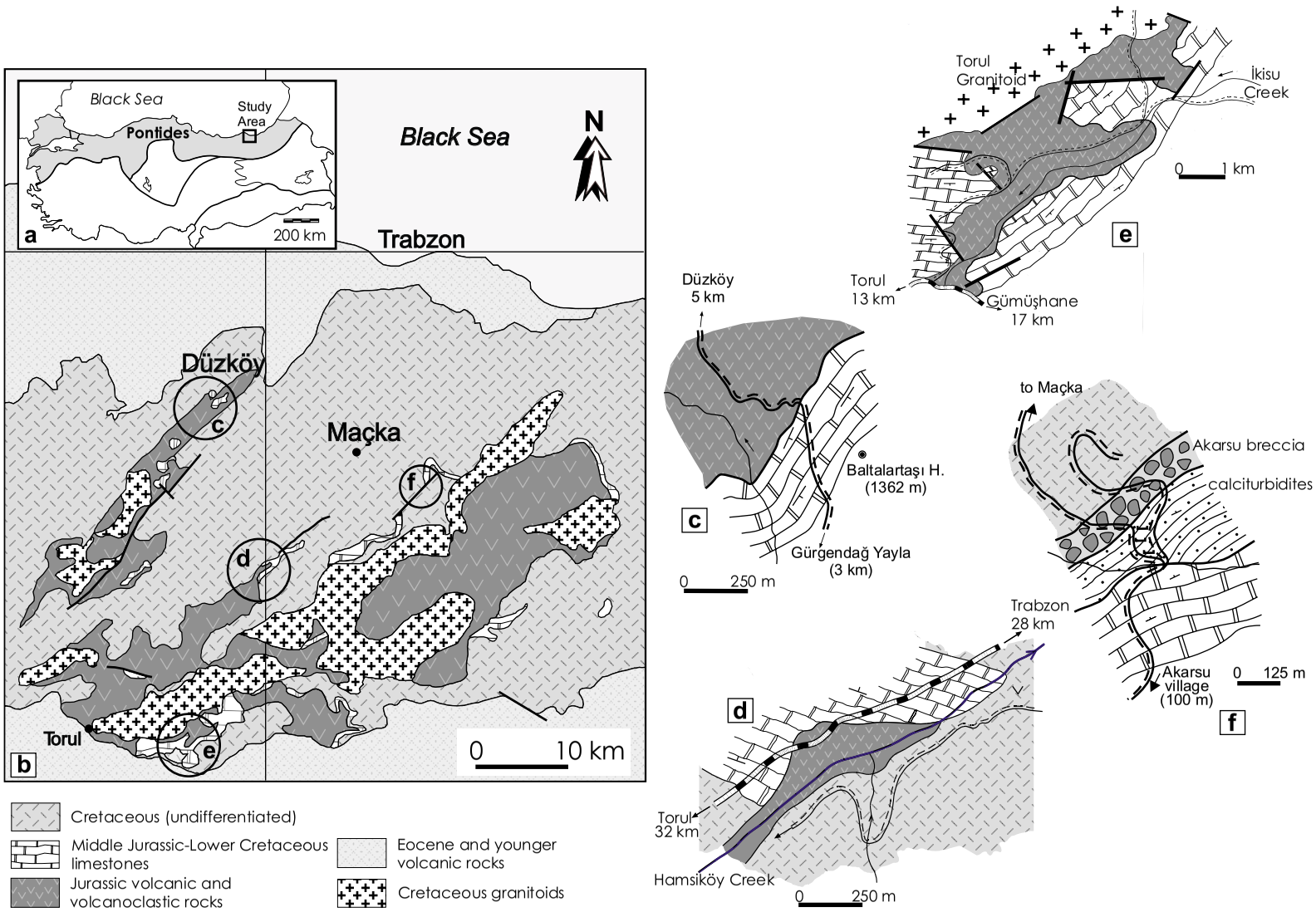

Figure 1. (a) Schematic map showing the major tectonic units of Turkey, (b) simplified geological map of the centre of the north zone of the eastern Pontides, sketch maps of studied locations: (c) Düzköy Gürgendağ Yayla, (d) Zigana Başarköy, (e) İkisu Valley; (f) and Akarsu.

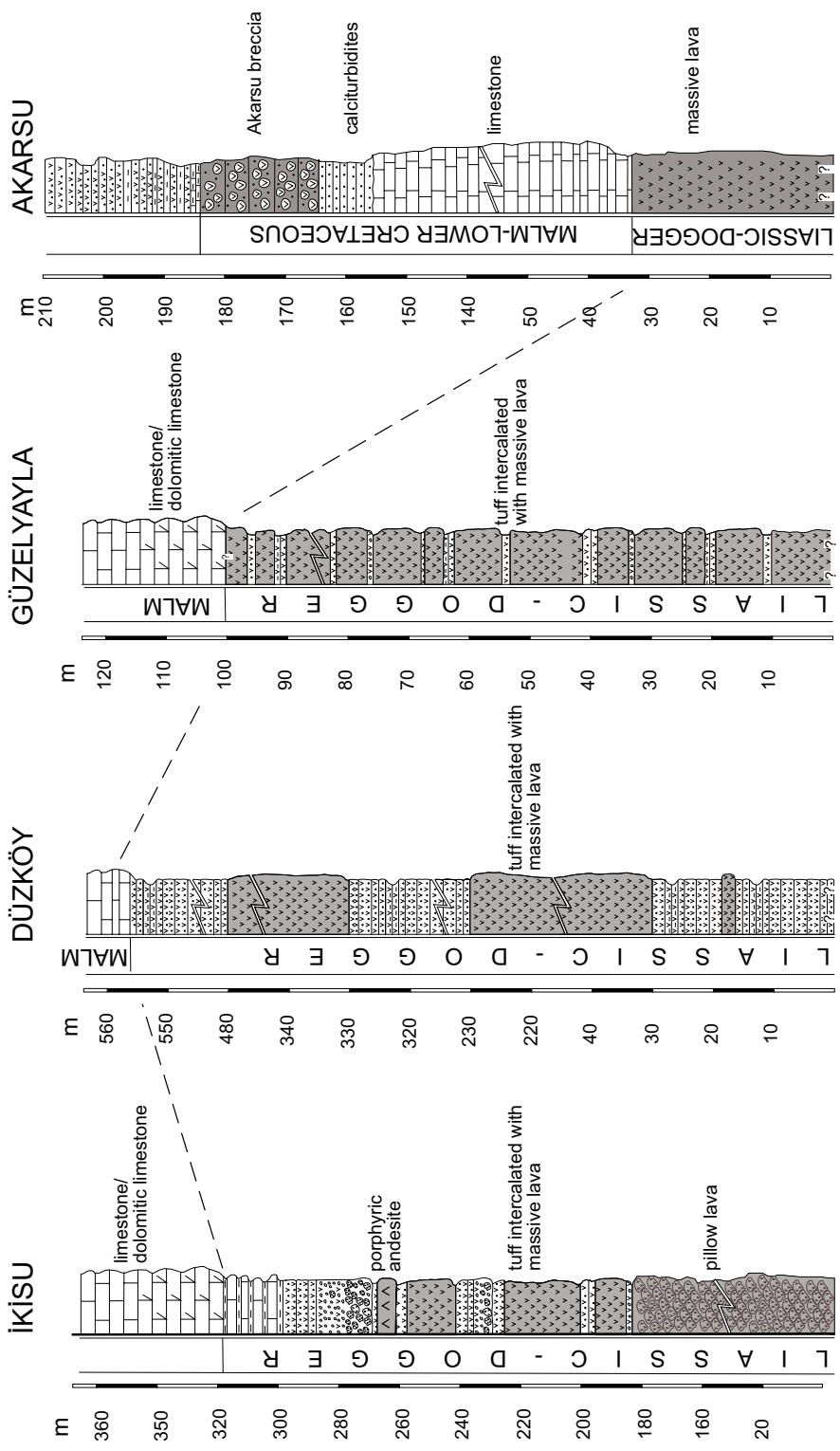

Figure 2. Stratigraphic sections from the studied locations.

and are themselves locally overlain by porphyritic andesite, containing plagioclase phenocrysts up to 2 cm long. Overlying epiclastic rocks with increasing carbonate content conformably grade up into carbonate platform rocks comprising thick-bedded limestones interbedded with dolomites and dolomitic limestones. On the basis of scarce benthic foraminiferal assemblages, this formation is assigned to the Middle Jurassic to Lower Cretaceous (Taslı 1984; Yalçıanalp 1992; Kurt *et al.* 2005). All these units are cut by the Torul granitoid (Kaygusuz 2000).

The stratigraphic sections at Başarköy (Zigana) and Gürgendağ Yayla (south of Düzköy) are similar to each other (Figure 2). Here, pyroclastic rocks intercalated with dark, aphyric to sparsely porphyritic (less than 5% phenocrysts) and amygdaloidal lavas, make up the basement. Thick, massive/bedded limestones overlie the basement volcanic sequence. Yılmaz & Korkmaz (1999) suggested that the volcanic rocks and overlying limestones are allochthonous mega-blocks which are locally interpreted as a para-autochthonous unit.

Although the stratigraphical section of Akarsu (east of Maçka, Figure 2) is almost the same as that measured at Başarköy and Gürgendağ, samples were collected from the blocks of breccia that stratigraphically overlies the carbonate platform. Both laterally and vertically the carbonates pass into calciturbidites, then volcano-silicic clastic rocks, and/or marl-siltstone and/or basic to intermediate volcanic rocks. In the Akarsu location, calciturbidites displaying a thinning and fining-upward sequence from bottom to top, unconformably overlie the carbonate platform limestones (Figure 2). Almost all the constituents of the calciturbidites originated from the carbonate platform and are defined as graded grainstone. They also include benthic and pelagic fossils (e.g., Hedbergella sp. *Texularia* sp., *Radiolaria* sp, from Kurt *et al.* 2005). These fossil contents indicate sudden foundering of the Jurassic to Mid Cretaceous carbonate platform during Albian to Aptian time. Calciturbidites, which form a key marker horizon throughout the Pontides, are considered to provide firm tectono-sedimentological evidence indicating the break-up of the carbonate platform (Yılmaz 2006; Yılmaz & Kandemir 2006).

Near the top, calciturbidites pass up into a monogenic breccia composed of basaltic to dacitic blocks (with rare marble blocks). The breccia is approximately 20 metres thick. The pale breccia is well sorted and consists of angular to semi-rounded porphyritic lava fragments ranging in size from a few cm's to 30 cm across, with pyroxene and plagioclase phenocrysts. The matrix of the breccia is compositionally almost the same as the calciturbidites. At the top of the unit, the breccia passes into an epiclastic facies composed of sandstone, siltstone, marl and tuff. It is suggested that, as calciturbidite deposition occurred during the break-up of carbonate platform, the basin was also supplied by detritus derived from the Jurassic volcanic rocks.

Petrography and Mineralogy

The volcanic sequence of the İkisu area is largely represented by pillow basalts and basaltic andesites. Nevertheless, some basaltic massive lava flows and porphyritic andesite flows occur in the upper part of the pillowed series. The pillow lavas exhibit aphyric to variably plagioclase-phyric texture; the groundmass is intersertal to subophitic, with laths of plagioclase and interstitial clinopyroxene. Quartz-filled amygdules were observed in a few samples from the upper part of the sequence. Massive lavas are represented by moderately porphyritic basaltic andesites, with clinopyroxene and minor plagioclase phenocrysts set within an intergranular groundmass of clinopyroxene and plagioclase microlites. Large (up to 1.5 cm) plagioclases with minor clinopyroxene characterize the porphyritic andesite. Disseminated subhedral Fe-Ti oxides are present in these rocks. All rock types are altered; common alteration products are albite, actinolite-tremolite, chlorite, epidote, prehnite, calcite, quartz, biotite, albite and minor calcite (replacing plagioclase) and actinolite (replacing clinopyroxene).

The volcanic rocks of Başarköy and Gürgendağ Yayla are mainly basaltic and andesitic lavas and tuffs, which have been extensively altered. The samples show microlitic to porphyritic textures. The basic rocks consist mainly of albitized plagioclase (An_{25-35}) and minor amounts of hypidiomorphic augite and idiomorphic Fe-Ti oxides. Microcrystalline plagioclase, augite and magnetite make up the intergranular to cryptocrystalline groundmass. Secondary alteration is more intensive in these rocks and sericite, prehnite, biotite, epidote and minor pumpellyite, together with calcite and silica varieties, fill veinlets and vesicles or replace primary phenocrysts.

The Akarsu samples were collected from the blocks of the breccia. The basaltic to andesitic blocks are porphyritic and are characterized by large (up to 1 cm) augite, and amphibole (up to 0.5 cm and found only in sample A-4) phenocrysts and slightly albitized plagioclase (An_{25-35}) with minor idiomorphic Fe-Ti oxides. Microcrystalline plagioclase, augite and Fe-Ti oxides make up the intergranular to cryptocrystalline groundmass. Sericite, epidote and calcite fill vesicles or partly replace primary minerals.

Analytical Methods

Thirty-one samples (12 from the İkisu Valley, 7 from Başarköy, 6 from Gürgen Yayla and 6 from the breccia blocks in the Akarsu area) were analysed for whole rock major-, trace- and rare earth element compositions by using ICP-emission spectrometry and ICP-Mass spectrometry using natural rock standards as reference samples for calibration at ACME Analytical Laboratories Ltd, Vancouver, Canada (Table 1). Major and trace elements were analysed by ICP on pulps after 0.2 g of rock-powder was fused with 1.5 g $LiBO_2$ and then dissolved in 100 ml 5% HNO_3. Loss on ignition (LOI) is by mass difference after ignition at 1000 °C. Rare earth element analyses were performed by ICP-MS on pulps after 0.25 g rock-powder was dissolved with four acid digestions. Detection limits range 0.01–0.1 wt% for major oxides, 0.1–10 ppm for trace elements and 0.01–0.5 ppm for the rare earth elements. A duplicate rerun of GT-1 is also given in Table 1 as GT-1b, to show analytical sensitivity.

Sr-Rb and Sm-Nd isotopic analyses were performed at IGG (Beijing). Details of the analytical methods can be found in the studies of Chen & Jahn (2004) and Chen & Arakawa (2005).

Results

Major and Trace Element Geochemistry

Major and trace element analyses of rock samples are presented in Table 1. SiO_2 content (49–64 wt% on anhydrous base) indicates that the rocks analysed are mainly basaltic andesites with minor basalts, andesite and dacite (sample A-4 only). Total alkalies have scattered values ranging from 2.5 to 7.5% (on anhydrous bases) and show a weak positive correlation with SiO_2. Microscope observations suggested that most rocks experienced the extensive low-grade metamorphism that is commonly observed in coeval rocks in the region. Because most of the studied samples have been altered and metamorphosed, their major element compositions may have been modified, so relatively immobile trace elements such as Ti, Zr, Hf, Y, Ta and REE have been used to deduce their tectonic environment.

In the Zr/TiO_2-Nb/Y diagram (Winchester & Floyd 1977) these rocks plot in sub-alkaline basalt, basaltic-andesite and andesite fields (Figure 3a). Zr/Y ratios were used to identify the geochemical affinity of the volcanic rocks, which in turn helps constrain the geodynamic setting. According to Barrett & MacLean (1997), Zr/Y ratios > 7 are calc-alkaline, <4 tholeiitic and between 4 and 7 transitional. Employing these relationships, samples are plotted on Figure 3b. The rocks investigated define an evolutionary trend from tholeiitic to transitional affinity. Some of the Akarsu and İkisu samples are tholeiitic, with the former having elevated Zr and Y values, probably due to fractional crystallization.

The large ion lithophile elements (LILE) generally show a higher dispersion than the high field strength elements (HFSE) due to their high mobility during alteration. However, despite the dispersion, some correlations were observed. Although most LIL elements are strongly dispersed, positive correlation of SiO_2 with Zr, Nb, Th, Hf and La was observed. The compatible elements Cr, Ni, V and Sc show a negative correlation with SiO_2, with a major dispersion in the case of Cr and Ni and a relatively high correction factor for V and Sc. Low Ni and Cr contents are in agreement with low MgO values.

Trace elements, normalized against normal mid-ocean ridge basalts (N-MORB) using the factors of Sun & McDonough (1989), show a typical pattern of subduction zone magmatism (Figure 4), with enrichments in some LILE (e.g., Rb, Ba) and depletions in relatively HFSE (e.g., Zr, Ti, Y) with respect to N-MORB. The general patterns of all four locations show great similarities (Figure 4). The patterns are characterized by an increase from Rb to Sr and a general decrease in P to Lu. In all samples, Pb shows a positive anomaly whereas Nb-Ta constitutes a negative anomaly where the Nb values are greater than 1.0 in all localities, but Ta is less than 1 in most samples. The volcanic rocks exhibit significant Nb depletion relative

Table 1. Major and trace element analyses for Jurassic volcanic rocks of the eastern Pontides.

	A-4 D	A-11 A	A-13 BA	A-17 A	A-23 B	A-24 A	GT-1 B	GT-1b B	GT-2 BA	GT-3 B	GT-4 BA	GT-5 BA	GT-6 B	ZL-1 BA	ZL-4 B	ZL-5 B
SiO_2	64.41	58.24	52.83	58.37	49.18	55.84	51.45	51.77	56.48	50.47	55.84	56.09	48.88	54.06	50.36	51.61
TiO_2	0.55	1.21	0.71	1.20	1.17	1.15	1.61	1.62	1.08	1.69	1.13	1.19	1.45	1.68	1.12	1.65
Al_2O_3	15.43	18.61	16.96	15.76	18.87	18.46	16.88	17.17	18.48	17.94	19.39	19.33	18.09	16.98	17.15	16.69
Fe_2O_3*	5.34	8.24	7.51	10.98	12.38	9.72	9.97	10.11	9.88	10.25	7.22	8.85	10.75	10.30	11.96	12.28
MgO	3.12	3.50	3.52	4.01	6.99	2.93	4.15	3.08	3.83	3.97	2.73	2.42	5.40	3.82	5.65	4.45
MnO	0.04	0.07	0.08	0.15	0.21	0.17	0.17	0.19	0.10	0.12	0.07	0.05	0.10	0.21	0.18	0.16
CaO	6.95	5.82	14.41	4.43	8.37	7.52	10.52	10.74	6.17	10.40	7.12	5.36	10.58	7.72	6.32	6.19
Na_2O	3.16	3.85	3.15	4.67	2.57	3.66	2.65	2.69	3.56	2.35	2.64	2.90	3.85	3.57	5.54	5.06
K_2O	0.85	0.36	0.68	0.12	0.11	0.30	2.12	2.15	0.25	2.29	3.47	3.39	0.54	1.26	1.22	1.37
P_2O_5	0.15	0.11	0.16	0.32	0.14	0.24	0.49	0.49	0.17	0.53	0.39	0.42	0.37	0.40	0.51	0.55
TOTAL	100	100	100	100	100	100	100	100	100	100	100	100	100	100	100	100
Cr_2O_3	0.042	0.005	0.009	0.004	0.003	0.005	0.009	0.009	0.006	0.008	0.022	0.014	0.057	0.006	0.011	0.008
LOI	2.10	4.80	7.80	4.80	5.40	2.80	7.70	7.70	3.00	7.50	8.30	7.20	7.30	10.40	6.90	6.00
Ba	173	244	156	114	141	127	234	236	114	225	158	167	109	64	266	271
Sc	16	17	18	16	39	27	19	19	26	20	19	21	25	24	31	20
Co	12	18	16	22	34	18	21	20	23	21	21	27	41	27	46	24
Pb	3.1	2.3	2.4	2.6	2.5	4.5	16.0	15.9	3.3	19.8	3.6	4.1	2.2	7.0	4.4	4.1
Zn	18	20	42	104	101	84	42	43	92	75	43	47	27	60	88	67
Ni	21.6	24.4	24.1	21.8	23.9	21.2	25.4	26.2	23.0	26.2	49.6	61.5	54.0	28.0	48.0	24.0
Cs	0.2	0.4	0.2	0.2	0.2	0.1	1.8	2.1	0.5	1.7	3.1	2.3	0.7	2.2	0.3	0.3
Ga	19.7	11.0	19.3	17.7	21.5	21.7	18.3	18.2	20.0	18.9	18.6	20.3	16.4	18.1	20.8	16.9
Hf	2.8	1.5	2.9	3.8	1.5	2.9	4.1	3.9	3.4	4.4	3.7	4.5	3.0	3.7	5.2	4.7
Nb	4.4	3.4	3.1	5.1	3.1	5.9	13.1	14.4	5.5	14.9	14.1	15.2	6.9	13.0	17.3	17.7
Rb	9.8	23.2	11.2	9.1	11.5	14.6	35.9	38.3	2.9	38.9	43.4	44.1	5.8	41.9	14.9	22.2
Sr	990	253	1187	476	303	431	334	330	726	367	213	224	568	147	516	410
Ta	0.2	0.1	0.1	0.3	0.2	0.2	0.7	0.9	0.3	0.8	0.7	0.9	0.3	0.6	1.0	1.0
Th	1.6	1.4	2.3	2.5	1.6	1.5	2.8	4.0	2.7	3.1	4.3	3.2	2.7	3.3	2.5	5.2
U	0.7	0.2	0.7	0.8	0.2	0.4	1.0	1.4	0.6	1.1	1.0	1.1	0.5	0.9	1.0	1.3
V	203	167	241	194	406	198	200	204	186	350	178	194	327	83	312	269
Zr	97	56	100	132	50	92	170	174	161	185	164	170	126	157	218	223
Y	16	24	16	33	19	30	31	32	30	32	24	26	29	31	40	32
La	11.60	19.50	16.30	19.10	8.20	12.40	25.70	26.40	13.10	26.60	28.20	27.70	15.40	20.80	27.50	31.80
Ce	25.00	28.78	35.70	42.20	17.20	28.20	54.50	57.20	27.20	58.80	58.50	56.60	37.50	53.70	59.20	66.60
Pr	3.36	3.77	4.00	5.15	2.10	3.44	6.50	6.65	3.36	7.19	6.19	6.40	4.40	5.95	7.53	8.06
Nd	14.50	15.80	17.20	22.60	9.90	16.20	27.70	29.20	15.90	31.00	24.70	27.40	19.70	29.30	38.10	37.90
Sm	3.30	3.00	3.50	5.60	2.70	3.90	6.00	5.90	4.00	6.60	5.40	5.60	4.50	5.30	7.50	7.40
Eu	0.92	0.67	1.10	1.55	0.96	1.31	1.72	1.71	1.27	1.92	1.51	1.43	1.63	1.53	2.07	1.87
Gd	2.63	2.93	2.87	5.16	3.08	4.50	5.60	5.52	4.60	6.12	4.70	4.93	4.71	5.23	6.84	6.29
Tb	0.47	0.52	0.51	0.90	0.56	0.70	0.90	0.91	0.79	0.96	0.73	0.79	0.78	0.82	1.24	0.94
Dv	2.86	3.47	3.48	5.41	3.02	4.70	5.03	5.41	4.84	5.38	4.40	4.98	4.85	4.74	6.22	5.42
Ho	0.61	0.73	0.74	1.08	0.67	1.02	1.11	1.11	1.07	1.16	0.90	1.05	1.06	1.01	1.55	1.03
Er	1.77	2.08	2.12	3.08	1.89	2.93	3.03	3.12	2.95	3.14	2.44	3.03	2.88	2.88	4.18	3.03
Tm	0.26	0.31	0.33	0.46	0.27	0.44	0.45	0.46	0.41	0.45	0.36	0.41	0.40	0.47	0.64	0.47
Yb	1.65	1.94	2.05	2.92	1.82	2.77	2.86	2.94	2.57	2.61	2.18	2.60	2.46	2.84	3.99	3.26
Lu	0.24	0.29	0.31	0.42	0.26	0.42	0.43	0.44	0.38	0.39	0.32	0.39	0.35	0.46	0.54	0.45

Table 1. Continued.

SiO_2	52.29	49.93	49.92	51.10	54.76	47.45	51.37	52.66	52.12	49.81	51.79	51.41	53.00	57.88	58.87	59.86
TiO_2	1.22	1.60	1.43	1.05	0.92	1.11	1.46	0.58	1.51	1.56	1.09	1.12	1.31	0.67	0.58	0.57
Al_2O_3	17.60	16.73	17.52	17.61	17.84	17.74	17.75	19.12	18.02	17.27	16.39	17.43	18.57	16.80	17.25	18.34
Fe_2O_3*	9.02	11.46	11.19	10.07	10.79	11.29	9.79	8.99	9.40	10.74	9.83	9.50	8.96	8.40	8.11	7.28
MgO	5.16	6.92	6.37	6.38	4.51	6.03	2.85	5.24	4.78	6.99	5.94	6.14	4.67	5.13	3.72	3.41
MnO	0.25	0.15	0.15	0.19	0.21	0.13	0.03	0.13	0.07	0.18	0.12	0.10	0.11	0.11	0.09	0.07
CaO	7.67	8.25	9.09	8.72	4.28	13.54	9.00	9.47	10.46	10.14	9.76	9.67	8.54	5.04	4.81	4.06
Na_2O	4.33	3.80	3.45	4.02	5.98	2.42	4.92	3.46	2.72	2.19	4.02	3.22	3.39	3.36	3.39	3.37
K_2O	2.17	0.93	0.47	0.69	0.58	0.10	2.55	0.25	0.56	0.56	0.66	0.99	1.23	2.32	2.98	2.94
P_2O_5	0.28	0.21	0.40	0.18	0.13	0.18	0.29	0.11	0.37	0.55	0.40	0.42	0.22	0.27	0.20	0.10
TOTAL	100	100	100	100	100	100	100	100	100	100	100	100	100	100	100	100
Cr_2O_3	0.019	0.038	0.014	0.008	0.002	0.022	0.018	0.005	0.041	0.005	0.008	0.006	0.005	0.002	0.002	0.002
LOI	9.60	9.40	4.20	3.80	4.00	7.80	8.70	7.90	7.80	2.20	4.40	3.30	4.16	3.75	3.98	3.90
Ba	367	67	155	326	219	57	157	184	57	82	208	184	231	272	298	377
Sc	21	35	28	39	30	31	26	30	26	20	28	34	32	28	25	24
Co	26	40	20	38	26	40	25	32	30	37	30	28	36	24	28	25
Pb	9.6	4.4	4.8		7.5	1.6	3.6	5.6	2.5	21.0	9.0	193.0	17.0	317.0	217.0	432.0
Zn	61	63	75		110	49	48	69	36	122	101	193	79	195	211	369
Ni	43.0	71.0	97.0	10.0	22.0	99.0	79.0	35.0	159.0	84.0	79.0	88.0	54.0	21.0	16.0	15.0
Cs	0.5	0.6	1.8	0.3	0.9	0.3	2.1	1.2	2.2	2.0	1.5	2.0	2.1	1.4	1.2	1.4
Ga	15.4	17.8	18.7	18.1	17.9	14.6	17.5	16.0	16.6	21.0	23.4	26.1	28.0	24.2	25.3	21.7
Hf	4.2	3.3	2.7	3.2	1.3	2.0	3.6	1.4	2.8	3.5	3.2	3.5	3.2	2.9	2.9	2.7
Nb	12.6	6.5	6.3	11.8	1.3	2.0	3.6	1.4	2.8	3.5	3.2	3.5	3.2	2.9	2.9	2.7
Rb	34.0	18.4	23.7	4.7	16.7	0.8	26.8	8.5	7.8	4.6	6.4	17.0	20.0	32.0	44.0	51.0
Sr	200	257	330	703	546	384	381	216	260	547	473	491	427	366	409	370
Ta	0.6	0.4	0.2	0.6	0.2	0.2	0.7	0.2	0.4	0.5	0.3	0.4	0.3	0.2	0.3	0.2
Th	4.5	1.3	2.5	2.1	1.5	0.7	2.0	3.7	1.8	3.2	2.4	3.4	2.5	1.8	2.0	1.7
U	1.3	0.3	0.5	0.3	0.5	0.3	0.4	1.2	0.4	0.9	0.8	1.0	0.8	1.4	1.5	1.6
V	154	256	283	222	253	177	133	196	183	154	184	168	172	138	149	151
Zr	180	119	96	127	57	87	142	53	127	158	120	112	158	141	137	83
Y	34	30	29	28	23	24	24	14	28	18	28	17	22	21	18	17
La	20.70	9.10	14.70	23.60	9.20	8.90	17.70	10.90	15.30	24.00	22.00	34.00	42.00	44.00	38.00	34.46
Ce	45.40	21.10	31.10	51.70	21.40	19.65	36.30	22.40	37.90	58.00	37.20	61.00	74.00	70.00	57.00	64.70
Pr	5.60	2.95	3.97	6.56	2.57	2.78	4.61	2.39	4.55	8.78	5.20	8.53	7.11	8.11	7.31	6.87
Nd	26.30	14.70	18.80	28.50	12.10	12.20	19.20	10.60	17.13	19.30	18.40	20.40	25.90	21.50	17.20	26.28
Sm	5.00	3.70	4.60	5.30	3.10	2.80	3.80	2.44	4.80	5.89	4.10	5.80	4.89	5.94	5.34	4.85
Eu	1.51	1.27	1.12	1.81	0.94	1.02	1.28	0.71	1.58	2.48	1.98	3.02	1.20	1.48	2.13	2.04
Gd	5.39	4.64	4.28	5.30	3.65	3.80	4.83	2.84	5.23	6.73	4.64	5.61	4.63	4.80	5.88	6.11
Tb	0.87	0.87	0.78	0.79	0.62	0.65	0.83	0.45	0.87	1.06	0.77	0.94	0.69	0.85	0.99	0.99
Dv	5.26	4.99	4.44	4.34	3.83	3.93	4.46	2.81	4.53	5.97	4.65	4.98	3.67	5.61	5.77	5.77
Ho	1.04	0.92	0.92	0.89	0.84	0.85	0.95	0.60	0.96	1.13	0.94	1.02	0.74	1.04	1.07	1.05
Er	3.26	3.05	2.82	2.65	2.36	2.35	2.61	1.75	2.77	2.73	2.67	2.67	2.03	2.81	2.78	2.79
Tm	0.50	0.46	0.46	0.38	0.34	0.33	0.39	0.24	0.40	0.36	0.41	0.36	0.32	0.42	0.39	0.37
Yb	3.03	2.97	2.81	2.44	2.14	2.18	2.36	1.57	2.36	2.35	2.46	2.19	1.68	2.67	2.31	2.09
Lu	0.45	0.40	0.40	0.38	0.30	0.29	0.31	0.23	0.34	0.31	0.35	0.29	0.25	0.35	0.33	0.28

A– andesite; B– basalt; BA– basaltic -andesite; D– dacite; PA– porhyritic andesite

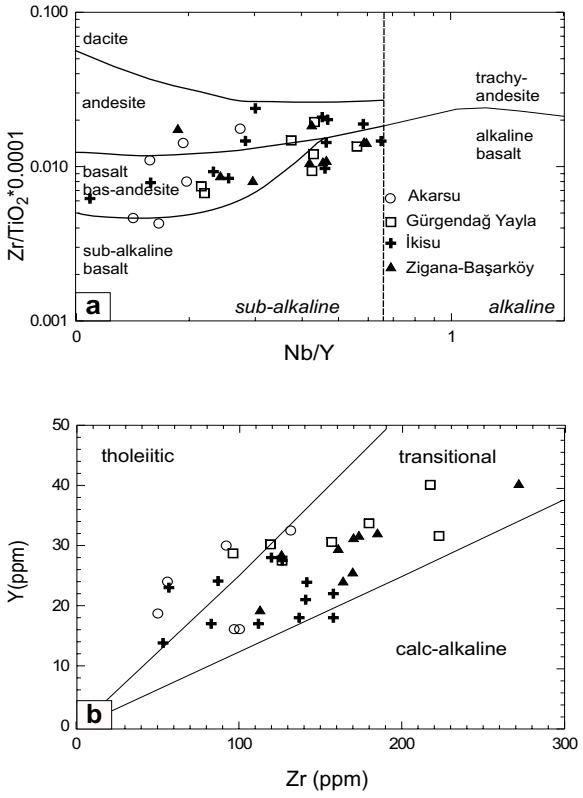

Figure 3. (a) Zr/TiO_2 vs Nb/Y (after Winchester & Floyd 1977) and, (b) Y vs Zr (Barrett & MacLean 1997) diagrams.

to La, with $(Nb/La)_n$= 0.10 – 0.77. In all samples Ti, Dy, Y, Yb and Lu present values close to, or slightly lower than, N-MORB.

The enrichment in LILE and LREE with positive Pb and (Sr) and negative Nb, Ta and Ti anomalies, may reflect either the introduction of a subduction component from the downgoing slab or crustal contamination through assimilation-fractional crystallization (AFC) and/or melting, assimilation, storage and homogenization (MASH) processes (Deniel 1998; Kerrich *et al.* 1999).

The rare earth element (REE) contents normalized against chondrite show a homogeneous pattern, with enrichment in light REE (La to Sm) with respect to heavy REE (Figure 5). Except for the İkisu porphyritic andesites (samples I-22; I-27 and I-35), the volcanic rocks exhibit relatively subparallel patterns, with ratios of $(La/Lu)_N$ 3 to 9; $(La/Sm)_N$ 2 to 6 and $(Lu)_N$ 7 to 14. Sub-parallel patterns imply that these magmas may have experienced shallow level crystal fractionation. But, no significant positive Eu anomalies were observed: the rocks have a slight negative Eu anomaly (with the exception of sample A-11), with the Eu/Eu* ratio ranging from 0.8 to 1.0. In general, the higher REE values correspond to samples richer in SiO_2. The İkisu porphyritic andesites contain higher REE contents than the other volcanic rocks and are characterized by recognizable positive Eu anomalies (Eu/Eu* ratios range 1.2 to 1.6, Figure 5)

Pearce *et al.* (1999) noted that, because Hf bulk distribution coefficients are intermediate between those of Nd and Sm for melts in equilibrium with residual spinel lherzolite, decoupling of REE and HFSE behavior due to subduction, or other higher-level process may be indicated by a positive or negative Eu anomaly in a chondrite normalized REE pattern. As seen in Figure 5, where Hf is plotted between Nd and Sm, most samples from Zigana and İkisu, and some samples from Akarsu exhibit a negative Hf anomaly. Pearce *et al.* (1999) stated that negative Hf anomalies were a characteristic of fore-arc lavas.

Isotope Geochemistry

Sr and Nd isotope ratios of the Eastern Pontide Jurassic rocks appear in Table 2 (only two samples, I22 and ZL 5, belong to the northern zone of the Eastern Pontides, the others are all from the southern zone of the eastern Pontides). Corrected for post-crystallization in-situ growth of radiogenic Sr and Nd compositions are also given in Table 2 and plotted in Figure 6. The $(^{87}Sr/^{86}Sr)_t$ (εNd_t is taken as 210 Ma for the calculations) ratios range 0.704570 to 0.705450 where as the $(^{143}Nd/^{144}Nd)_t$ ratios range 0.5122376 – 0.512579 ($\varepsilon Nd(210\ Ma)$= -0.72 to 3.24).

Discussion

Characteristics of the volcanic rocks can generally be attributed to: (1) various amounts of assimilation, fractional crystallization of mantle-derived magma and crustal contamination *en route*; (2) various degrees of partial melting of a homogeneous source at different pressures and temperatures; and (3) mantle source variability, e.g. metasomatised lithospheric mantle or hybridized source (Bell & Simonetti 1996). Here, characteristics of investigated volcanic rocks are tested according to the attributions above.

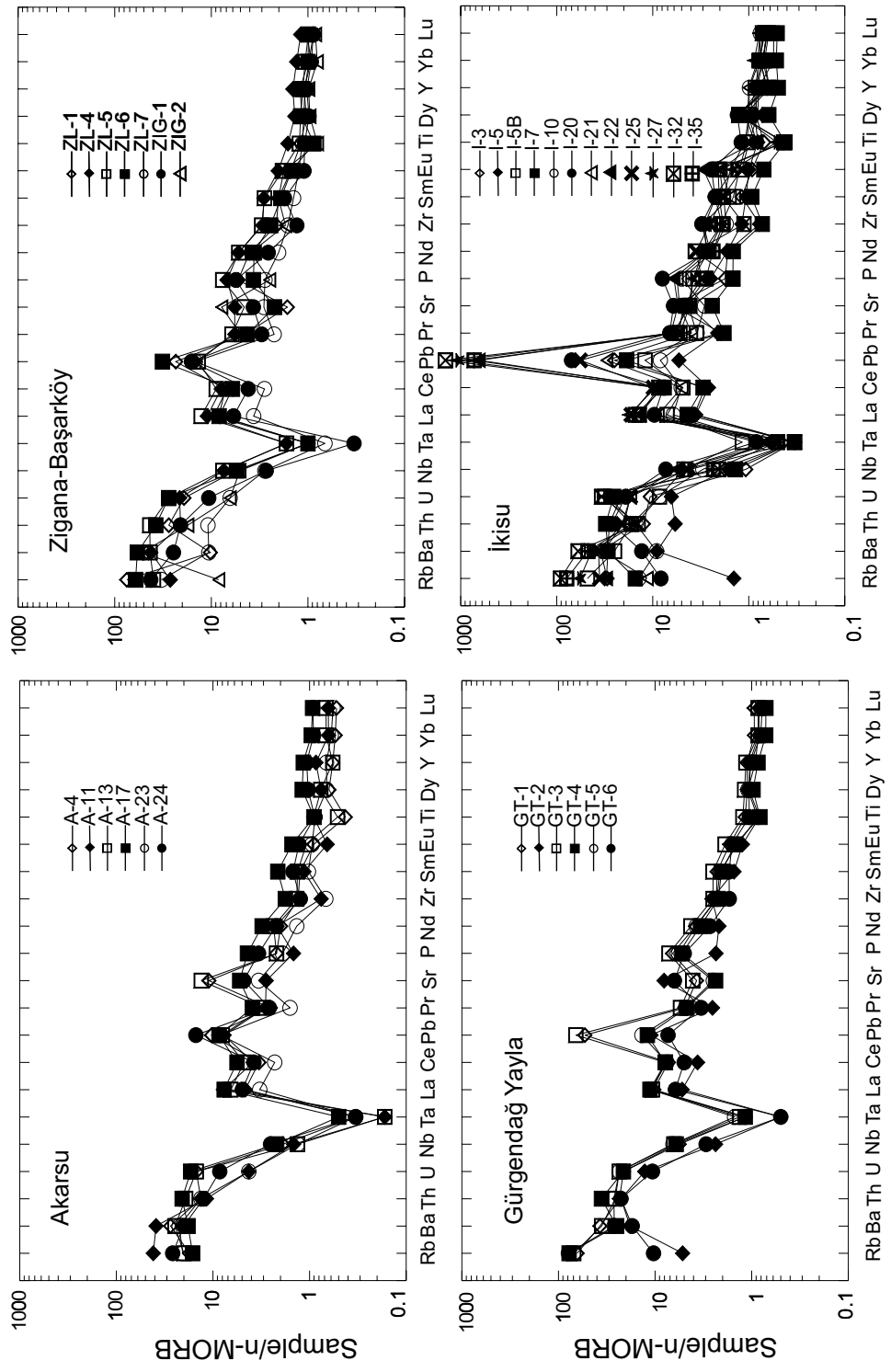

Figure 4. N-MORB normalized trace element patterns for Jurassic volcanic rocks of studied locations. Normalizing values are from Sun & McDonough (1989).

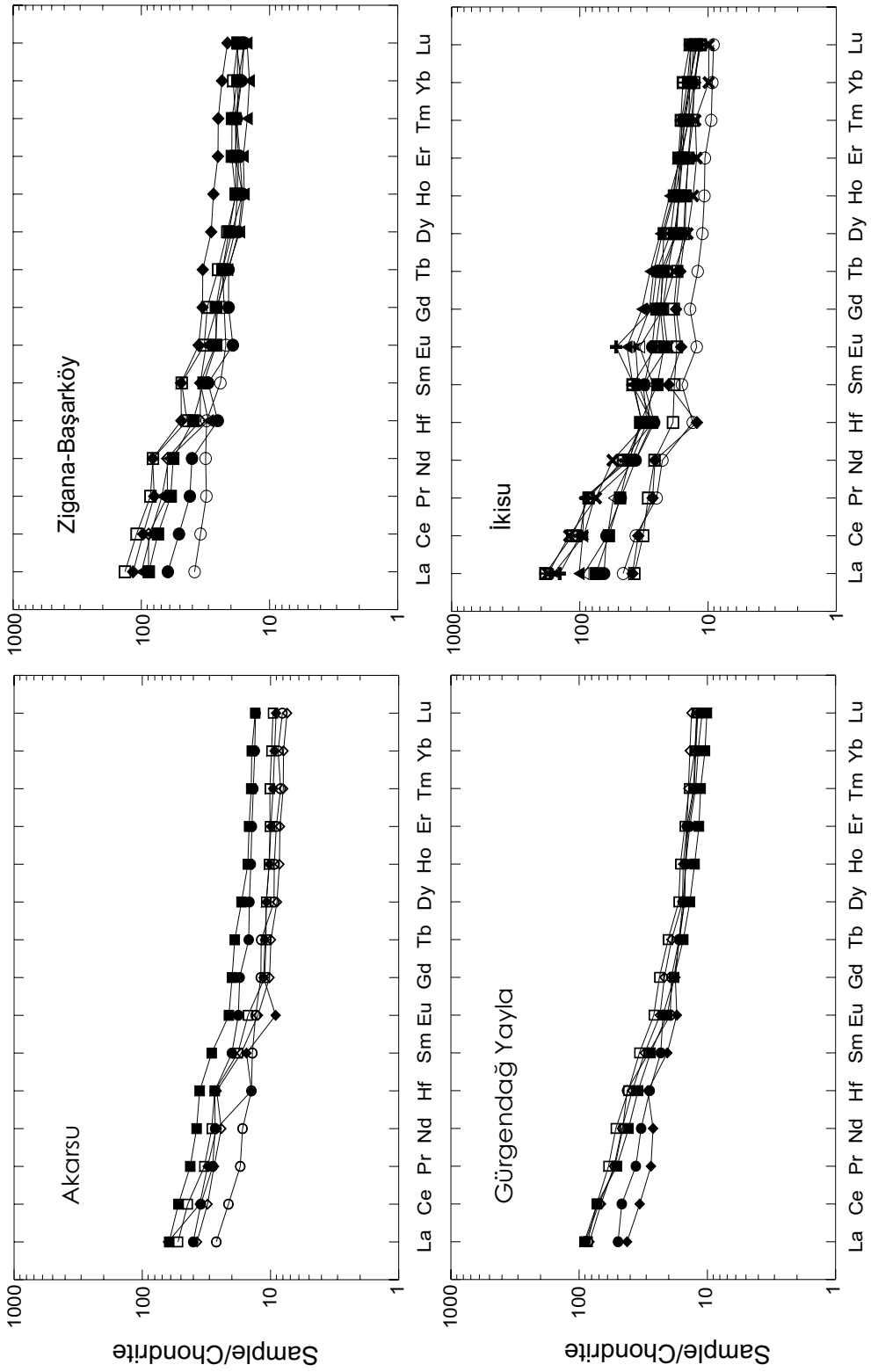

Figure 5. Chondrite-normalized REE and Hf patterns of Jurassic volcanic rocks of the north zone of the eastern Pontides. Normalizing values are from Sun & McDonough (1989).

Table 2. Sr-Nd isotopic analyses for Jurassic volcanic rocks of the eastern Pontides.

Sample No.	Rb (ppm)	Sr (ppm)	Sm (ppm)	Nd (ppm)	$^{87}Rb/^{86}Sr$	$(^{87}Sr/^{86}Sr)_0$	$^{147}Sm/^{144}Nd$	$(^{143}Nd/^{144}Nd)_0$	$(^{87}Sr/^{86}Sr)_t$	$(^{143}Nd/^{144}Nd)_t$	$(\varepsilon Nd)_t$
P3	22.11	612.2	8.370	42.24	0.1039	0.705263(11)	0.1200	0.512586(12)	0.705004	0.512447	0.70
TL14	7.335	317.0	2.956	11.54	0.0665	0.705172(13)	0.1551	0.512669(12)	0.705006	0.512491	1.54
I22*	23.46	564.8	5.124	25.23	0.1197	0.704868(11)	0.1230	0.512621(13)	0.704570	0.512480	1.32
U29	18.48	525.4	3.783	17.03	0.1011	0.705702(11)	0.1345	0.512530(21)	0.705450	0.512376	-0.71
ZL5*	20.08	391.9	6.408	31.22	0.1480	0.705601(12)	0.1242	0.512721(13)	0.705232	0.512579	3.24
BCR-1	46.69	330.5	6.671	28.65	0.4081	0.705003(11)	0.1410	0.512624(19)			

Uncertainties (in brackets) are ±2– within run precision and refer to the last digits.
εNd_t calculated using chondritic reference (CHUR) with present parameters $^{143}Nd/^{144}Nd$= 0.512638 and $^{147}Sm/^{144}Nd$=0.1967

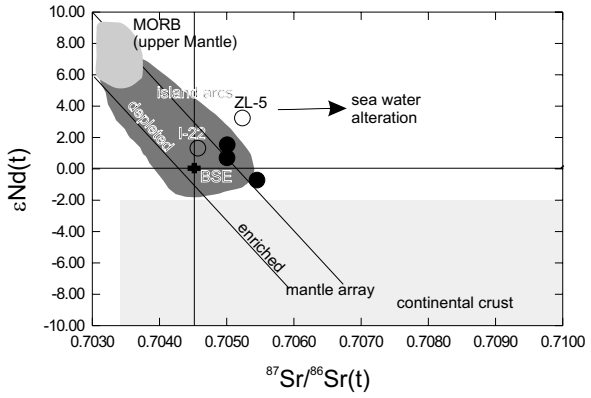

Figure 6. εNd(210 Ma) vs $^{87}Sr/^{86}Sr$(210 Ma) diagram for samples from the Jurassic rocks of the eastern Pontides. Mantle Array according to DePaolo & Wasserburg (1979); BSE-Bulk Silika Earth.

Alteration Effects

Alteration to various degrees of the volcanic rocks in the region can be determined from petrographic observations and relatively high loss on ignition in almost all the samples (2.20 – 8.01%). Some incompatible elements, such as Rb, Ba and K, are known to be mobile during weathering (e.g., Bach *et al.* 1999), as demonstrated by the considerable scatter in the primitive-mantle-normalized patterns shown in Figure 4. The age-correction of measured $^{87}Sr/^{86}Sr$ involves Rb concentrations, and thus their effect on initial $^{87}Sr/^{86}Sr$ ratios is particularly important. However, the consistency demonstrated by the data set (except for Rb and Ba) in primitive-mantle-normalized patterns (Figure 4), suggests that absolute abundances and ratios of incompatible elements, such as REE, Th, U, Nb, Ta, Zr, Hf, Y, Ti, are the least sensitive to weathering. This is supported by a large number of studies (Jochum *et al.* 1991; Deniel 1998; Kerrich *et al.* 1999). Accordingly, the following discussions focus on these immobile elements and εNd(t) value.

Crustal Contamination and Magma Fractionation

The rocks have high Th content and Th/Ta ratios of 2.5 – 23.0 (avg. 7.5 ± 4.3, Table 1), but relatively constant $(Nb/La)_N$ (avg. 0.47 ± 0.17) , $^{87}Sr/^{86}Sr(_t)$ ratios and $\varepsilon Nd(_t)$ values irrespective of SiO_2 content (Tables 1 & 2). This suggests that these rocks encountered little to no crustal contamination during their ascent (Kramer *et al.* 2005). The broad similarity in immobile incompatible element behaviour for all samples also suggests negligible crustal contamination *en route* through the crust (Kramer *et al.* 2005).

The studied samples do not represent primary melts (i.e. low Mg#, Ni and Cr concentrations). These characteristics, shown on REE and trace element diagrams, suggest that the magma underwent a degree of fractional crystallization in magma chambers prior to extrusion at the surface.

Hart & Davis (1978) reported that the Cr/Ni ratios of arc basalts are approximately 2.0, and their concentrations at 11.0% MgO (primitive arc basalt) are 640 and 320 ppm, respectively. Olivine and clinopyroxene have the highest partition coefficient for Ni and Cr among silicates. Fractionation of these minerals must result in a drastic depletion in a residual magma. The effect of continuous fractionation of olivine and clinopyroxene has been calculated to explain the main trend for Cr and Ni in the studied samples. The range of Cr and Ni concentrations in the studied samples can be explained by separation of 12–25% olivine and 4–10% clinopyroxene (Figure 7).

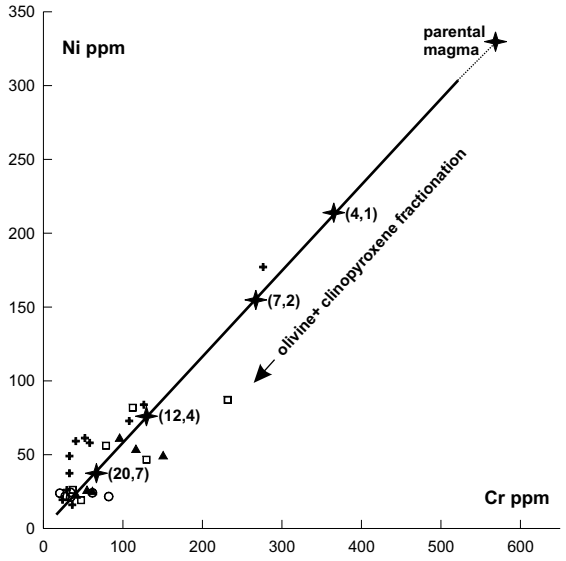

Figure 7. Plot of Ni and Cr concentrations in studied volcanic rocks. The solid line indicates linear regression of Ni and Cr concentrations (r= 0.89) and the assumed path of olivine and clinopyroxene fractionation. Stars on the line indicate selected degrees of fractionation and numbers brackets refer to the amount of fractionated phases, e.g. (4; 1) means fractionation of 4% olivine and 1% clinopyroxene.

These lavas lack distinct Eu anomalies (except for the porphyric andesites the average Eu/Eu* ratio is 0.94) suggesting very little, if any, fractionation of plagioclase. Because Si, Ca and Na concentrations have probably changed during alteration, a check of plagioclase fractionation using major elements is impossible. However, fractionations of large amounts of calcic plagioclase must also result in a significant decrease in the Al abundance of the residual melts. Some samples have higher Al_2O_3 contents, indicating that plagioclase fractionation must play a subordinate role, if at all.

In summary, it is concluded that the moderate separation of olivine and clinopyroxene can explain the observed range of Cr and Ni concentrations. The role of plagioclase has been of minor importance.

Degree of Partial Melting

In general, low La/Yb ratios reflect a melting regime dominated by relatively large melt fractions and/or spinel as the predominant residual phase, whereas high La/Yb ratios are indicative of smaller melt fractions and/or garnet control. Therefore, relatively low $(La/Yb)_N$ and $(Gd/Yb)_N$ ratios, combined with relatively moderate HREE abundance, in these volcanic rocks suggests that they may have formed by low degrees of partial melting of a spinel-bearing source. The relatively low P_2O_5/Al_2O_3 ratios (0.006–0.033) for these rocks also indicate a relatively low percentage of melting. However, the ratios of incompatible elements with similar distribution coefficients (e.g., Th/Nb, Zr/Nb, Nb/La), which are the least susceptible to partial melting and fractional crystallization processes, show regular variation, as illustrated in Table 1. Such variations in incompatible element ratios and isotopic compositions potentially suggest that they were generated by variable degrees of partial melting of the same homogeneous source (Pearce 1983).

Tectonic Setting

As discussed previously, the tectonic setting of the Jurassic volcanic rocks of the eastern Pontides is still debated, with two distinct models proposed. One suggests rift-related volcanism (e.g., Şengör & Yılmaz 1981; Görür *et al.* 1983; Bergougnan 1987), and the other argues for subduction related volcanism (e.g., Kazmin *et al.* 1986; Golonka 2004).

Trace element (negative Nb-Ta, Ti, Zr anomalies in Figure 4) and isotope data (depleted εNd values in Figure 6) appear to support a subduction-related cause of the volcanism, rather than rifting.

Combined use of Sr and Nd isotope ratios can be a particularly powerful geochemical tool. Figure 6 shows the Sr and Nd isotopic characteristics of major terrestrial reservoirs and the studied samples. Most of the mantle has εNd higher than, and $^{87}Sr/^{86}Sr$ lower than bulk silica earth (BSE). MORB and most island arc basalts tend to have low $^{87}Sr/^{86}Sr$ and high εNd values. $^{87}Sr/^{86}Sr8_{(t)}$ and $\varepsilon Nd_{(t)}$ values of the studied samples plot in the εNd depleted and $^{87}Sr/^{86}Sr$ enriched sector of the diagram. As discussed above, sea water alteration may cause the Sr enrichment in the rocks. Nevertheless, the isotopic characteristics of the studied samples are comparable with those of island arc volcanic rocks (Kramer *et al.* 2005).

Bailey (1981) recognized four types of andesite settings: oceanic island arcs that are divided into low-K and 'other' andesites, continental island arcs, thin continental margins and thick continental margins

(Andean). All these andesites could be discriminated using a La/Yb vs Sc/Ni plot and by high contents of Al, low contents of Ti, Zr, REE, Y, Nb, Ta and Ga, and the absence of pronounced negative Eu anomalies. Using Bailey's (1981) trace element criteria, the tectonic setting of these Jurassic volcanic rocks were tested on La/Yb-Sc/Ni diagram (Figure 8). La/Yb ratios in volcanic rocks are good indicators of the mantle source. On the other hand, increasing Sc/Ni ratios can be caused by increased crustal contamination of the magmas. Most of the samples fall within a narrow Sc/Ni range (≥ 1) and plot in the continental arc field. The same tectonic setting can be proposed using the Th/Yb-Ta/Yb discrimination diagram (Figure 9). According to the original boundaries proposed by Pearce (1983), Jurassic volcanic rocks from the Eastern Pontides belong to an active continental margin.

Conclusions

All these investigations indicate that the Jurassic volcanic rocks of the northern zone of the Eastern Pontides represent a suite of active continental arc lavas, ranging from highly depleted basalt to dacite. The homogeneous isotopic geochemistry of these lavas, with slightly enriched initial Sr ratios (~ 0.7052) and depleted εNd values (-0.7 to 3.2) is typical of modern subduction-related magmas. Based on geochemical data (both trace element and isotopic signatures), an arc setting is therefore proposed for the Jurassic volcanic rocks from the centre of the northern zone of the eastern Pontides. However, evidence of a transtensional tectonic regime in the Pontides is shown by many researchers (Şengör & Yılmaz 1981; Görür *et al.* 1983; Bergougnan 1987; Yılmaz *et al.* 1996; Koçyiğit & Altıner 2002; Yılmaz 2006; Yılmaz & Kandemir 2006), and it is thought that this transtensional tectonic regime split the arc as an inter-arc rift. Kandemir (2004), Şen *et al.* (in prep) and this study propose a model in which south-facing half-grabens formed in the continental arc. The investigated volcanic rocks were located at the north end of the half graben and pyroclastic rocks were dominant in the north, while epiclastic rocks were dominant in the south (Figure 10).

Acknowledgements

The author would like to thank Ercan Aldanmaz for his thorough, critical and constructive reviews and

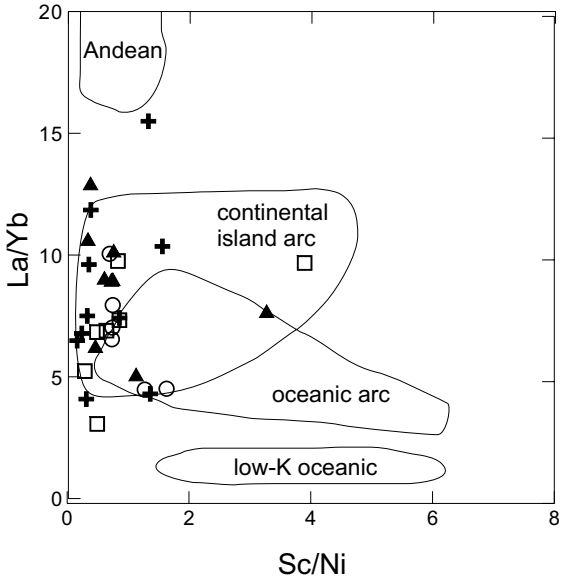

Figure 8. Discrimination diagram of La/Yb vs Sc/Ni (after Bailey 1981) for the Jurassic rocks of the eastern Pontides.

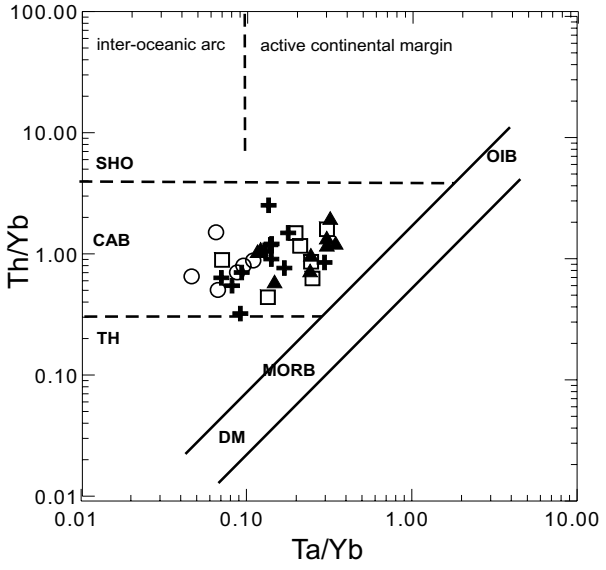

Figure 9. Th/Yb vs Ta/Yb diagram of Jurassic volcanic rocks according to Pearce (1983). The investigated rocks influenced by subduction components. DM– depleted mantle, MORB– mid-ocean ridge basalts, OIB– ocean island basalts, TH– tholeiite, CAB– calc-alkaline basalt, SHO– shoshonite.

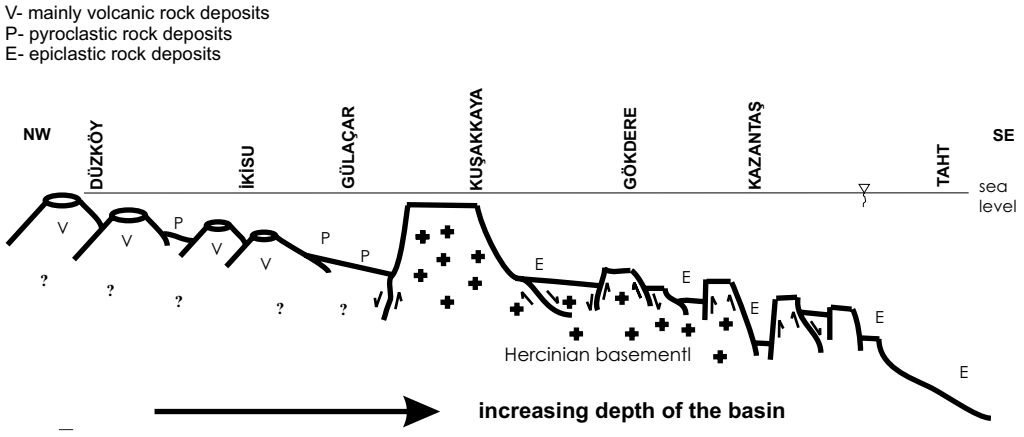

Figure 10. Sketch cross section (from Şen *et al.* 2007) illustrating possible relationship among the studied Jurassic basins and the Jurassic basins that are further south.

comments, and E. Bozkurt for his helpful editorial advice. I also thank C. Yılmaz (KTÜ) and İ. Kurt (MTA, Trabzon) for their critical and constructive comments. Thanks are also due to O. Karslı, F. Aydın and R. Kandemir for their help during field work. Financial support for this study was jointly provided by TÜBİTAK (YDABAG 103Y017) and Research Fund of Karadeniz Technical University (2003.112.005.5) grants. John A. Winchester helped with the English of the final text.

References

ADAMIA, S., LORDKIPANIDZE, M.B. & ZAKARIADZE, G.S. 1977. Evolution of an active continental margin as exemplified by the Alpine history of the Caucasus. *Tectonophysics* **40**, 183–189.

AKIN, H. 1978. Geologie, magmatismus und largerstaettenbildung im ostpontischen gebirge-Türkei aus der sicht der plattentektonik. *Geologische Rundschau* **68**, 253–283.

ARSLAN, Z. 2005. Petrography and petrology of the calc-alkaline Sarıhan Granitoid (NE Turkey): an example of magma mingling and mixing. *Turkish Journal of Earth Sciences* **14**, 183-207.

ARSLAN, Z. 2006. Reply to comment on 'petrography and petrology of the calc-alkaline Sarıhan Granitoid (NE Turkey): an example of magma mingling and mixing'. *Turkish Journal of Earth Sciences* **15**, 379–384.

BACH, W., ALT, C.J., NIU, Y., HUMPHRIS, E.S., ERZINGER J. & DICK H.J. 2001. The geochemical consequences of late-stage low-grade alteration of lower ocean crust at the SW Indian Ridge: results from ODP Hole 735B (Leg 176). *Geochimica et Cosmochimica Acta*, **65**, 3267–3287

BAILEY, J.C. 1981. Geochemical criteria for refined tectonic discrimination of orogenic andesites. *Chemical Geology* **32**, 139–154.

BARRETT, T.J. & MACLEAN W.H. 1997. Volcanic sequences, lithogeochemistry and hydrothermal alteration in some bimodal VMS systems. *In*: BARRIE, C.T. & HANNINGTON, M.D. (eds), *Volcanic-Associated Massive Sulfide Deposits: Process and Example in Modern and Ancient Settings*. Ottawa, Canada, 105–133.

BEKTAŞ, O., ŞEN, C., ATICI, Y. & KÖPRÜBAĞI, N. 1999. Migration of the Upper Cretaceous subduction related volcanism towards the back-arc basin of the Eastern Pontide magmatic arc (NE Turkey). *Geological Journal* **34**, 95–106.

BELL, K. & SIMONETTI, A. 1996. Carbonatite magmatism and plume activity: implication from the Nd, Pb isotope systematics of Oldoinyo Lengai. *Journal of Petrology* **37**, 1321–1339.

BERGOUGNAN, H. 1987. *Etudes geologiques dans l'est Anatolien*. PhD Thesis, Pierre et Marie Curie University, Paris-France.

CHEN, B. & ARAKAWA, Y. 2005. Elemental and Nd-Sr isotopic geochemistry of granitoids from the west Junggar foldbelt (NW China), with implication for Phanerozoic continental growth. *Geochimica Cosmochimica Acta* **69**, 1307–1320.

CHEN, B. & JAHN, B.M. 2004. Genesis of post-collisional granitoids and basement nature of the Junggar Terrane, NW China: Nd-Sr isotope and trace element evidence. *Journal of Asian Earth Sciences* **23**, 691–703.

DENIEL, C. 1998. Geochemical and isotopic (Sr, Nd, PB) evidence for plume-lithosphere interactions in the genesis of Grande Comore magmas (Indian Ocean). *Chemical Geology* **144**, 281–303.

DEPAOLO, D.J. & WASSERBURG, G.J. 1979. Petrogenetic mixing models and Nd-Sr isotopic pattern. *Geochimica Cosmochimica Acta* **43**, 615–627.

DEWEY, J.F., PITMAN III, W.C., RYAN, W.B.F. & BONNIN, J. 1973. Plate tectonics and the evolution of the Alpine system. *Geological Society of America Bulletin* **84**, 3137–3180.

DERCOURT, J., RICOU L.E. & VRINELYNCK, B. 1993. *Atlas of Tethys Palaeoenvironmental Maps*. Paris, Gauthier-Villars.

DOKUZ, A. & TANYOLU, E. 2006. Geochemical constraints on the provenance, mineral sorting and subaerial weathering of Lower Jurassic and Upper Cretaceous clastic rocks of the Eastern Pontides, Yusufeli (Artvin), NE Turkey. *Turkish Journal of Earth Sciences* **15**, 181–209.

GEDİKOĞLU, A., PELİN, S. & ÖZSAYAR, T. 1979. Tectonic evolution of the eastern Pontides in Mesozoic. *Geocome-I Abstracts*, p. 68

GOLONKA, J. 2004. Plate tectonic evolution of the southern magrin of Eurasia in the Mesozoic and Cenozoic. *Tectonophysics* **381**, 235–273.

GÖRÜR, N., TÜYSÜZ, O., AKYOL, A., SAKINÇ, M., YİĞİTBAŞ, E. & AKKOK, R. 1983. Cretaceous red pelagic carbonates of northern Turkey: their place in the opening history of the Black Sea. *Eclogae Geologicae Helvetiae* **36**, 819–838.

HART, S.R. & DAVIS, K.E. 1978. Nickel partitioning between olivine and silicate melt. *Earth and Planetary Science Letters* **40**, 203–219.

JOCHUM, K.P., ARNDT, P.N.T. & HOFMANN, A.W. 1991. Nb-Ta-La in komatiites and basalts: constraints on komatiite petrogenesis and mantle evolution. *Earth Planetary Science Letters* **107**, 272–289.

KANDEMİR, R. 2004. *Gümüşhane ve Yakın Yörelerindeki Erken–Orta Jura Yaşlı Şenköy Formasyonunun Çökel Özellikleri ve Birikim Koşulları [Sedimentary Characteristics and Depositional Conditions of Lower–Middle Jurassic Şenköy Formation in and around Gümüşhane]*. PhD Thesis, Karadeniz Technical University, Trabzon [in Turkish with English abstract, unpublished].

KAYGUSUZ, A. 2000. *Torul ve Çevresinde Yüzeylenen Kayaçların Petrografik ve Jeokimyasal İncelenmesi [Petrography and Geochemistry of Rocks Exposed in and Around Torul]*. PhD Thesis, Karadeniz Technical University, Trabzon [in Turkish with English abstract, unpublished].

KAZMIN, V.G., SBORTSHIKOV, I.M., RICOU, L.E., ZONENSHAIN, L.P., BOULIN, J. & KNIPPER, A.L. 1986. Volcanic belts as markers of the Mesozoic Cenozoic active margin of Eurasia. *Tectonophysics* **123**, 123–152.

KERRICH, R., POLAT, A., WYMAN, D. & HOLLINGS, P. 1999. Trace element systematics of Mg-, to Fe-tholeiitic basalt suits of the Superior Province: implications for Archean mantle reservoirs and greenstone belt genesis. *Lithos* **46**, 163–187.

KETİN, İ. 1966. Tectonic units of Anatolia. *Mineral Research and Exploration Institute (MTA) of Turkey Bulletin* **66**, 22–34.

KOÇYİĞİT, A. & ALTINER, D. 2002. Tectonostratigraphic evolution of the North Anatolian paleorift (NAPR): Hettangian–Aptian passive continental margin of the northern Neo-Tethys, Turkey. *Turkish Journal of Earth Sciences* **11**, 169–191.

KRAMER, W., SIEBEL, W., ROMER, R.L., HAASE, G., ZIMMER, M. & EHRLICHMANN R. 2005. Geochemical and isotopic characteristics and evolution of the Jurassic volcanic arc between Arica (18°30' S) and Tocopilla (22° S), North Chilean Coastal Cordillera. *Chemical Geology* **65**, 47–78.

KURT, İ., ÖZKAN, M., KARSLI, Ş. & ÇOLAK, T. 2005. *Keşap (Giresun)-Çarşıbaşı (Trabzon)-Torul (Gümüşhane) Arasının Jeolojisi [Geology of Keşap (Giresun)-Çarğıbaşı (Trabzon)-Torul (Gümüşhane) Region]*. Mineral Research and Exploration Institute (MTA) of Turkey Publications [in Turkish with English abstract.

OKAY, A.İ. 2000. Was the late Triassic orogeny in Turkey caused by the collision of an oceanic plateau? *In*: BOZKURT, E., WINCHESTER, J.A. & PIPER, J.D.A. (eds), *Tectonics and Magmatism in Turkey and the Surrounding Area*. Geological Society, London, Special Publications **173**, 25–41.

OKAY, A.İ., MONOD, O. & MONIE, P. 2002. Triassic blueschists and eclogites from northwest Turkey: vestiges of the Paleo-Tethyan subduction. *Lithos* **64**, 155–178.

OKAY, A.İ. & ŞAHİNTÜRK, Ö. 1997. Geology of the eastern Pontides. *In*: ROBINSON, A.G. (ed), *Regional and Petroleum Geology of the Black Sea and Surrounding Regions*. American Association of Petroleum Geologists Memoir **68**, 291–311.

ÖZSAYAR, T., PELİN S. & GEDİKOĞLU, A. 1981. Cretaceous in the eastern Pontides. *Black Sea Technical University Earth Science Bulletin* **1/2**, 65–114 [in Turkish with English abstract].

PEARCE, J.A. 1983. Role of the sub-continental lithosphere in magma genesis at active continental margins. *In*: HAWKESWORTH, C.J. & NORRY, M.J. (eds), *Continental Basalts and Mantle Xenoliths*. Shiva, Nantwich, 230–249.

PEARCE, J.A., KEMPTON, P.D., NOWELL, G.M. & NOBLE, S.R. 1999. Hf-Nd element and isotope perspective on the nature and provenance of mantle and subduction components in Western Pacific arc-basin systems. *Journal of Petrology* **40**, 1579–1611.

ROBERTSON, A.H.F. & DIXON, J.E. 1984. Introduction: aspects of the geological evolution of the eastern Mediterranean. *In*: DIXON, J.E. & ROBERTSON, A.H.F. (eds), *The Geological Evolution of the Eastern Mediterranean*. Geological Society, London, Special Publications **17**, 1–74.

ŞEN, C., YILMAZ, C., KAYGUSUZ, A., KARSLI, O., AYDIN, F., KANDEMİR, R., KURT, İ., 2007. *Doğu Pontid'lerdeki Jura Volkanitlerinin Jeokimyasal Özellikleri [Geochemical Characteristics of Jura Volcanics in Eastern Pontides]*. TÜBİTAK Project Report no. **103Y017** [in Turkish with English abstract, unpublished].

ŞENGÖR, A.M.C. 1987. Tectonics of the Tethysides: orogenic collage development in a collisional setting. *Annual Reviews Earth Planetary Sciences* **15**, 213–244.

ŞENGÖR, A.M.C. & YILMAZ, Y. 1981. Tethyan evolution of Turkey: a plate tectonic approach. *Tectonophysics* **75**, 181–241.

ŞENGÖR, A.M.C., YILMAZ, Y. & SUNGURLU, O. 1984. Tectonics of the Mediterranean Cimmerides: nature of evolution of the western termination of Paleotethys. *In*: DIXON, J.E. & ROBERTSON, A.H.F. (eds), *The Geological Evolution of the Eastern Mediterranean*. Geological Society, London, Special Publications **17**, 77–112.

SUN, S.S. & MCDONOUGH, W.F. 1989. Chemical and isotopic systematic of ocean basalts: implication for mantle composition and processes. *In*: SAUNDERS, A.D. & NORRY, M.J. (eds), *Magmatism in Ocean Basins*. Geological Society, London, Special Publications **42**, 313–345.

TASLI, K. 1984. Geology of Hamsiköy (Trabzon) area. *Black Sea Technical University Earth Science Bulletin* **1/2**, 69–76.

TOPUZ, G. 2006. Contact Metamorphism Around the Eocene Saraycık Granodiorite, Eastern Pontides, Turkey. *Turkish Journal of Earth Science* **15**, 75–94.

TOPUZ, G. & OKAY, A.İ. 2006. Comment on 'Petrography and petrology of the calc-alkaline Sarıhan Granitoid (NE Turkey): an example of magma mingling and mixing'. *Turkish Journal of Earth Sciences* **15**, 379–384.

USTAÖMER, T. & ROBERTSON, A. 1997. Tectonic-sedimentary evolution of the North Tethyan margin in the Central Pontides of Northern Turkey. *In*: ROBINSON, A.G. (ed), *Regional and Petroleum Geology of the Black Sea and Surrounding Regions.* American Association of Petroleum Geologist Bulletin Memoir **68**, 255–290.

WINCHESTER, J.A. & FLOYD, P.A. 1977. Geochemical discrimination of different magma series and their differentiation products using immobile elements. *Chemical Geology* **20**, 325–343.

YALÇINALP, B. 1992. *Geology and Geochemistry of the Porhyric Cu-Mo Ore Deposits in Güzel Yayla (Maçka, Trabzon)*. PhD Thesis, Karadeniz Technical University, Trabzon [in Turkish with English abstract, unpublished].

YILMAZ, C. 2006. Platform-slope transition during rifting: The mid-Cretaceous succession of the Amasya Region (Northern Anatolia), Turkey. *Journal of Asian Earth Sciences* **27**, 194–206.

YILMAZ, C. & KANDEMİR, R. 2006. Sedimentary records of the extensional tectonic regime with temporal cessation: Gümüşhane Mesozoic Basin (NE Turkey). *Geologia Carpathica* **57**, 3–13.

YILMAZ, C. & KORKMAZ, S. 1999. Basin development in the eastern Pontides, Jurassic to Cretaceous, NE Turkey. *Zentralblatt fur Geologie und Palaontologie*. Teil I **H10–12**, 1485–1494.

YILMAZ, C., ÖZGÜR, S. & TASLI K. 1996. Polygenic rifting phase records of the Mesozoic sediments in Gümüşhane region. *49th Geological Congress of Turkey* **11**, 170–175.

YILMAZ, C., ŞEN, C., CERYAN, Ş., KANDEMİR, R., KARSLI, O. & KARABAK, T. 2005. *Trabzon kıyı bölgesinin Pliyo-Kuvaterner Stratigrafisi [Quaternary stratigraphy of shoreline Area Around Trabzon].* Türkiye Kuvaterner Sempozyumu (TURQUA) **V**, 111–117.

YILMAZ, Y., TÜYSÜZ, O., YİĞİTBAŞ, E., GENÇ, Ş.C. & ŞENGÖR, A.M.C. 1997. Geology and tectonic evolution of the Pontides. *In*: ROBINSON, A.G. (ed), *Regional and Petroleum Geology of the Black Sea and Surrounding Regions*. American Association of Petroleum Geologists Memoir **68**, 183–226.

Received 04 September 2006; revised typescript received 21 February 2007; accepted 28 March 2007